Supporting Information for "Imaging widespread seismicity at mid-lower crustal depths beneath Long Beach, CA, with a dense seismic array: Evidence for a depth-dependent earthquake size distribution"

A. Inbal, R.W. Clayton , and J.-P. Ampuero
Seismological Laboratory, California Institute of Technology Pasadena, CA , USA.

Contents of this file

1. Text S1
2. Figures S1 to S4

1. Introduction

We present supporting material for the manuscript "Imaging widespread seismicity at mid-lower crustal depths beneath Long Beach, CA, with a dense seismic array: Evidence for a depth-dependent earthquake size distribution". The material contains three figures. The purpose of the figures is to illustrate the advantages of downward-continuing the data prior to back-projection, and to provide details on event detection and the robustness of earthquake rate calculation.

2. Downward Continuation

Figure S1 presents the mean amplitude in a 20 second time window recorded by the LB array. The raw data were filtered between 5-10 Hz, normalized by the 1-hour RMS of each trace, and interpolated on a grid whose cell size is 100x100 meters. The left and right panels in Figure S1 are for amplitudes of data at the surface, and for data that were downward-continued to a depth of 5 km. Note that downward-continuation significantly decreases the RMS of the data, as indicated by the histograms above each panel.

Figure S2 presents the results of a synthetic tests whose objective is to show that incorporation of downward-continuation allows us to recover the position of a source in poor signal-to-noise conditions. The left and right columns are for the synthetics at the surface, and for synthetics that were downward-continued to 5 km, respectively. Panels present stack maxima for a 10 second window containing a monochromatic, exponentially decaying signal. Noise is added to the signal by randomly distributing 100 uncorrelated, Gaussian noise sources at depths of 0-2 kilometres beneath the array. The input source is at a depth of 20 km, and its amplitude is 10% of the average surface noise level. In the top row the stack is averaged between 17.5 and 22.5 km. In the second row the stack is projected on a vertical plane oriented east-west. The bottom two panels show an example of a synthetic trace, where the expected arrival of the input signal in indicated by a red arrow. Note the input location (indicated by a cross) is recovered only after the data are downward-continued. Also note that in the bottom left panel the arrivals are indistinguishable from the noise, and thus would not have been identified by a standard STA/LTA detection algorithm.

3. Statistical Analysis of back-projection images

The detection procedure is carried out by analyzing the filtered, normalized, downward-continued, stacked envelopes. We stack (delay and sum) the envelopes of the downward continued waveforms for each potential position, window the stack for each position in our grid with 5-second, non-overlapping windows, construct a back-projection image from the peak amplitude of each window, and select the location that corresponds to the maximum of the image. We end up with a time-series containing the maxima of the back-projection image, on which the detection is made. Figure S3a shows the distribution of the logarithm of amplitudes of the migrated envelopes for a node located in the middle of our grid during one night of recordings. Figure S3b shows the distribution of the maxima in the 5-seconds windows for the same time period. Because the noise is log-normally distributed, the ensemble of observations containing its maxima belongs to Gumbel distribution.

A 5-second window is identified as containing a true event is its maximum amplitude exceeds a threshold corresponding to 5 times the MAD of the distribution of noise. This value allows us to determine the probability of false detections, which is the probability that a sample randomly drown from the ensemble of the stack maxima is actually noise. The probabilities can be computed based on the fact that the stack maxima belongs to a Gumbel distribution, but the signal we wish to detect is belongs to a power-law or exponential distributions. To estimate the probabilities we generate 1000 realizations of Gaussian noise whose variance is equal to the variance in the back-projection images, select the maxima of each realization, and use a maximum-likelihood estimator to fit the data to a Gumbel distribution. For a given threshold value T, the probability of false detection is estimated by using:

$$P = 1 - F(T; \mu, \beta), \tag{1}$$

where μ and β are the fitting coefficients. The rate of false alarms is obtained by multiplying the probability by the number of instances on which detection is preformed.

4. Synthetic tests of seismicity rate in a composite catalog

Because the static stress change decays rapidly with distance from each mainshock, areas that are within several tens of fault lengths away from the event see very small stress changes. The seismicity rate change is proportional to the stress step (*Dieterich* 1994; *Ziv et al.*, 2003), and is therefore small at the distances we consider in this analysis. Using a smaller distance bin is difficult because of computational limitations. It would require significant computational effort to reduce the grid to 0.1x0.1x0.1 km, already about 10 fault lengths away from each potential mainshock.

The seismicity rate is more likely to be affected by the maximum length of the time window used to compute the composite catalog (10 hours in our case). Due to the truncation, mainshocks occurring near the end of the night may appear to contain fewer aftershocks than early mainshocks. If the composite catalog is contaminated with apparently shorter sequences, that should cause the seismicity rate to approach the $1/t$ slope even faster, which will shorten the plateau in Figure 4d. Thus, the actual time it takes the seismicity rate to approach the $1/t$ curve may be even longer

0148-0227/15/$9.00

than what is shown in Figure 4d. We have compiled composite catalogs using no more than 8 hours each night, without much change to the results presented in Figure 4d.

The background seismicity rate is thought to obey a Poisson distribution. Figure S4 presents the earthquake rate as a function of time for a catalog in which event times are drawn from a Poissonian distribution. In these simulations, we truncate the catalog such that the latest manishock that may trigger aftershocks 5×10^3, 1×10^4, and 2×10^4 seconds less than the duration of the catalog. Rather than the expected constant rate, the truncation results in a spurious rate increase early in the sequence, and rapid decay late in the sequence. The duration of the plateau and the decay rate in the synthetic tests in Figure S4 are larger than what is observed for the LB catalog, which confirms that it is dominated by Omori-type clustering of aftershock sequences.

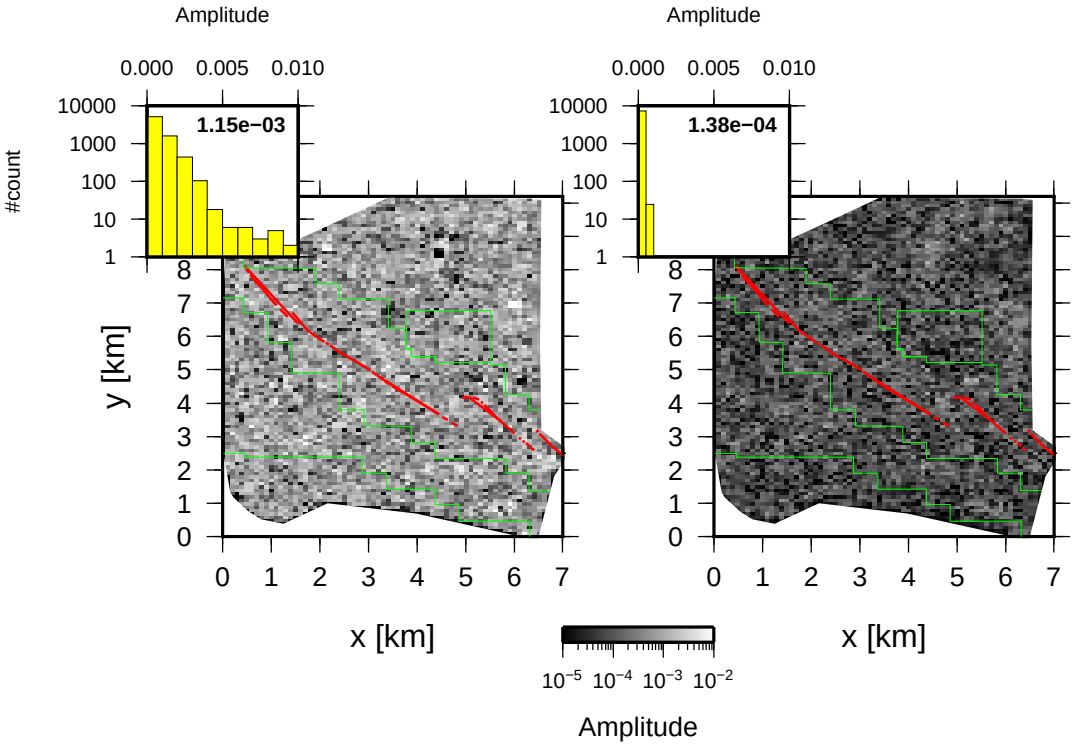

Figure S1. Mean amplitude of 20 second time window recorded by the LB array. Left: Surface recordings interpolated onto a 100x100 meter grid. Right: Surface recordings interpolated onto a 100x100 meter grid and downward continued to a depth of five km. Histograms and bold number indicate the amplitude distribution and RMS of each image. Red curve is for the NIFZ. Green polygons indicate to boundaries of active oil fields. Note that the RMS of the downward-continued data are about one order of magnitude smaller than the RMS of surface data.

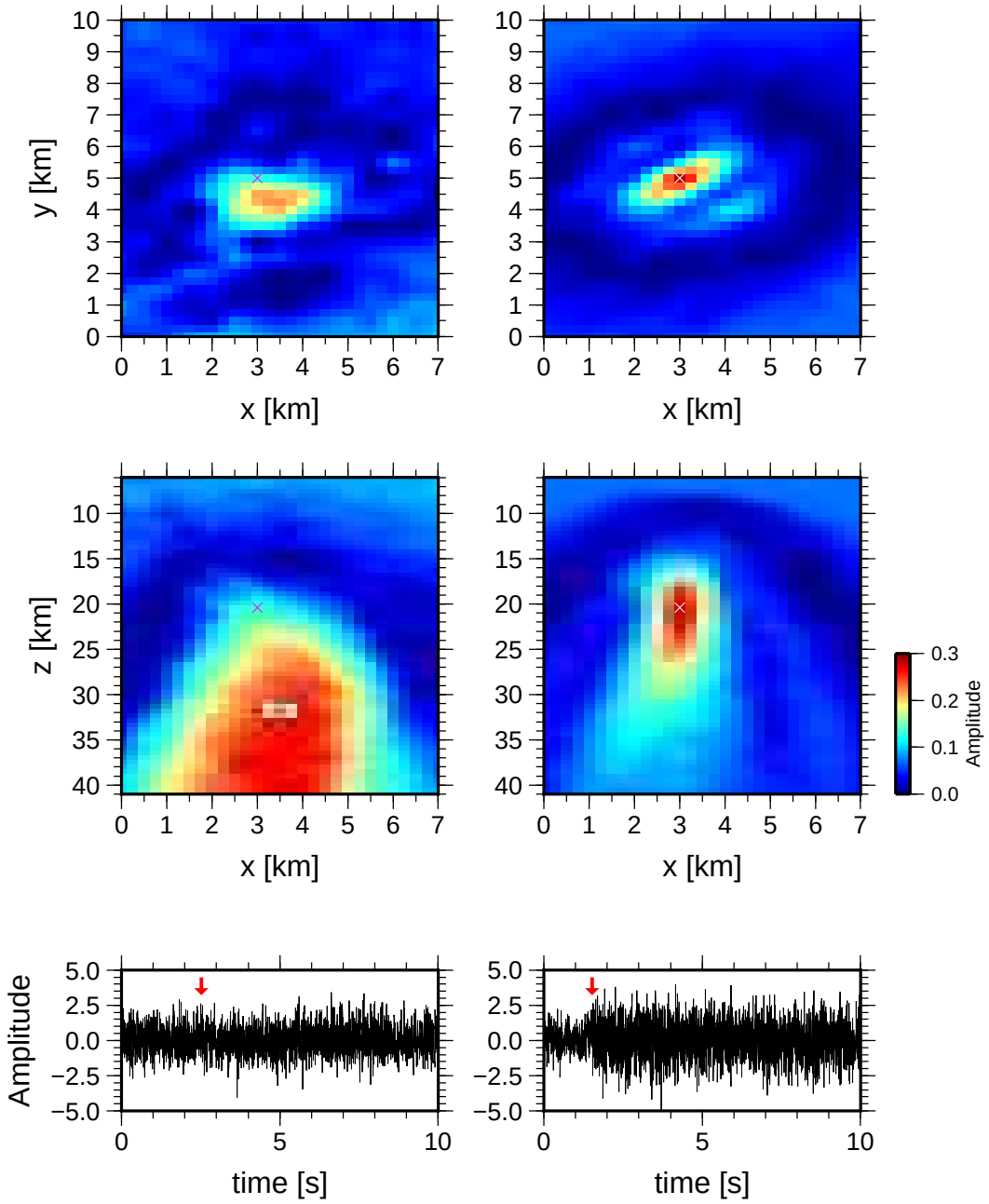

Figure S2. Back-projected stack amplitude as a function of position for synthetic tests. Source amplitude is 10% of average surface noise level. Cross indicates location of input. Left column: Data are back-projected from the surface. Right column: Data are downward-continued to 5 km and back-projected. Bottom panels shows the input synthetic at one of the sensors. Red arrow indicates the expected arrival time for an exponentially decaying monochromatic signal.

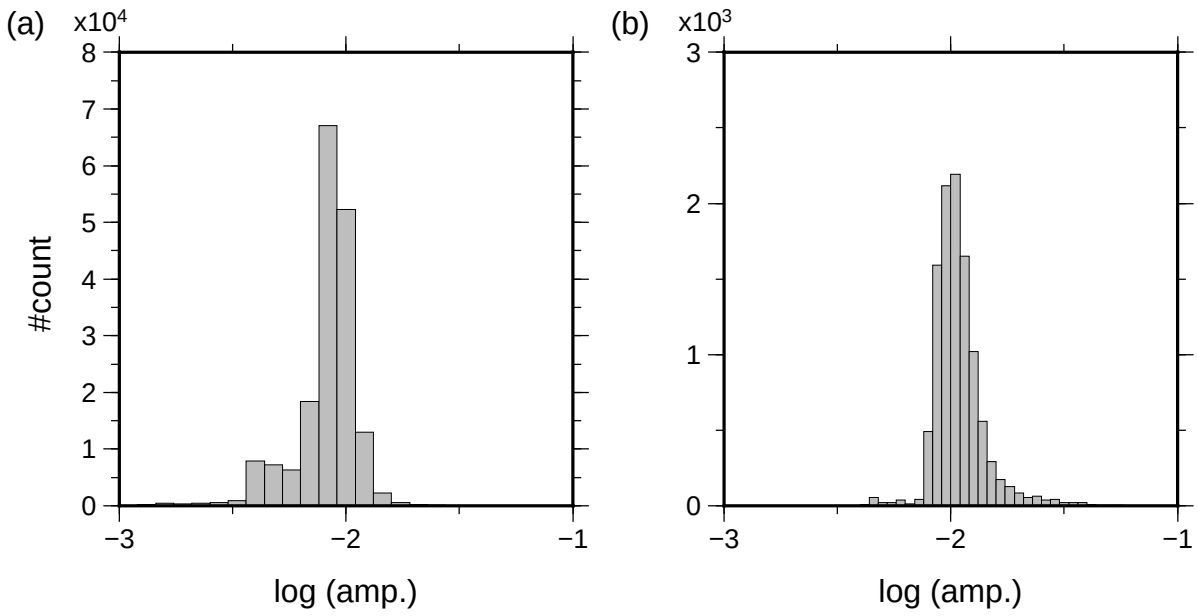

Figure S3. Amplitude distribution from one night of recordings. (a) Log amplitudes of stack at the center of the grid. (b) Peak log amplitude for 5-second windows.

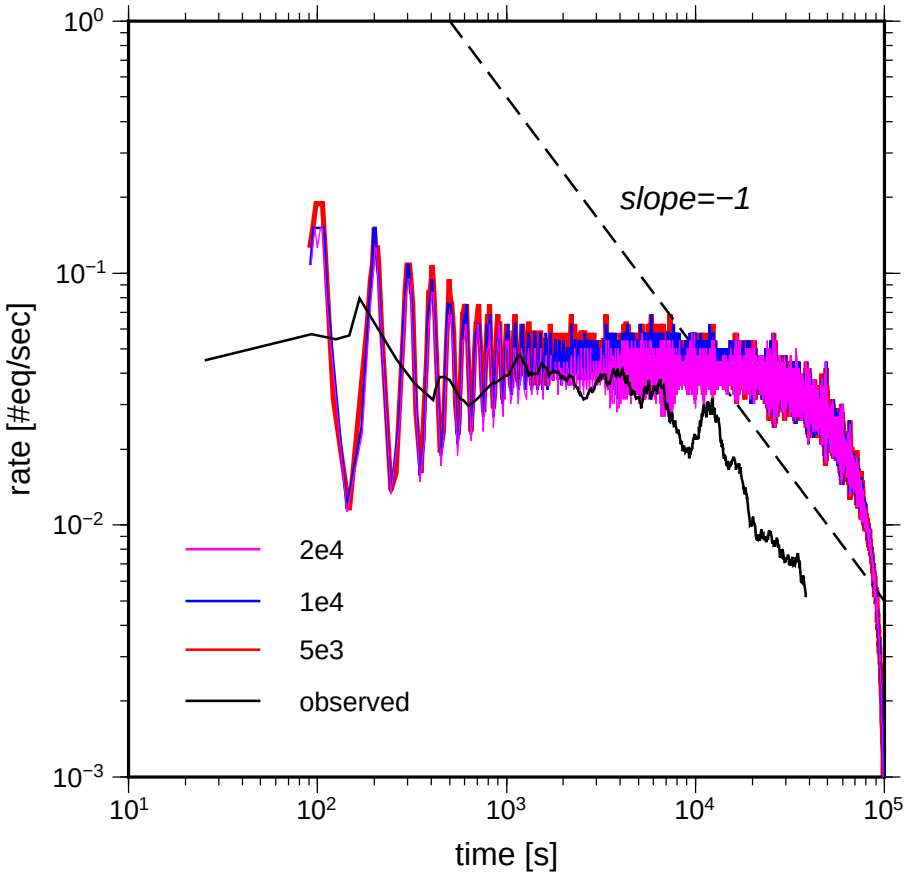

Figure S4. Rate of earthquakes as a function of time since mainshocks derived from a composite catalog. Black curve is for the observed seismicity rates. Red, blue, and magenta curves are for a synthetic catalog which was compiled for potential mainshocks that occur 5×10^3, 1×10^4, and 2×10^4 seconds less than the duration of the catalog, respectively. Dashed curve serves as reference for a $1/t$ Omori-like decay

.